# COMPARATIVE STUDY OF ELECTROMAGNETIC COUPLING ARCHITECTURES FOR VIBRATION ENERGY HARVESTING DEVICES

**D. Spreemann[1], B. Folkmer[1], Y. Manoli[1, 2]**
[1] Institute for Micromachining and Information Technology, HSG-IMIT, Villingen-Schwenningen, Germany
[2] Department of Microsystems Engineering, University of Freiburg, IMTEK, Freiburg, Germany

**Abstract:** In this paper five different commonly used electromagnetic coupling architectures in vibration energy harvesting devices are optimized in a construction volume of 1 cm³ using semi–analytical magnetic field calculations. The optimization goal is the maximum voltage as well as the maximum power output. Quantitative comparison of the architectures is presented. It is shown that for optimized conditions the maximum possible output voltage can be increased by a factor of two and the output power can be increased by a factor of three only by choosing a proper architecture. Experimental results obtained with a setup to measure the magnetic flux gradient are used to verify the simulation models.

**Key words:** Vibration energy harvesting, Electromagnetic coupling architecture, Optimization

## 1. INTRODUCTION

The effect of electromagnetic induction can be used to convert energy of different physical domains. In vibration energy harvesting applications mechanical energy (movement of an inertial mass) needs to be converted into electrical energy. Following Faraday's law of induction this can be obtained by producing a magnetic flux change in a closed loop of wire. In vibration transducers this is mostly realized by moving a magnet relative to a coil. This can be realized in various kinds. For this reason a lot of different architectures have been established and applied by numerous research facilities in the recent years. To the best of the authors knowledge a detailed realistic comparison on how much voltage and power can be obtained for the different architectures in a certain construction volume has not been published so far. In this paper we present a comparative study of five commonly used architectures (Fig. 1). They can be divided into two groups namely "Magnet in–line coil" and "Magnet across coil" architectures. Optimization calculation is applied to each architecture in order to optimize the voltage and power output.

Primarily, boundary conditions based on mesoscale vibration transducers are defined which are valid for all architectures. Afterwards each architecture is optimized in a construction volume of 1 cm³. For the optimization approach semi–analytical static magnetic field calculations are used. The investigated architectures consist of a permanent magnet (cylindrical or rectangular) and a cylindrical coil. The coil material is assumed to have no influence on the static magnetic field distribution. The optimal

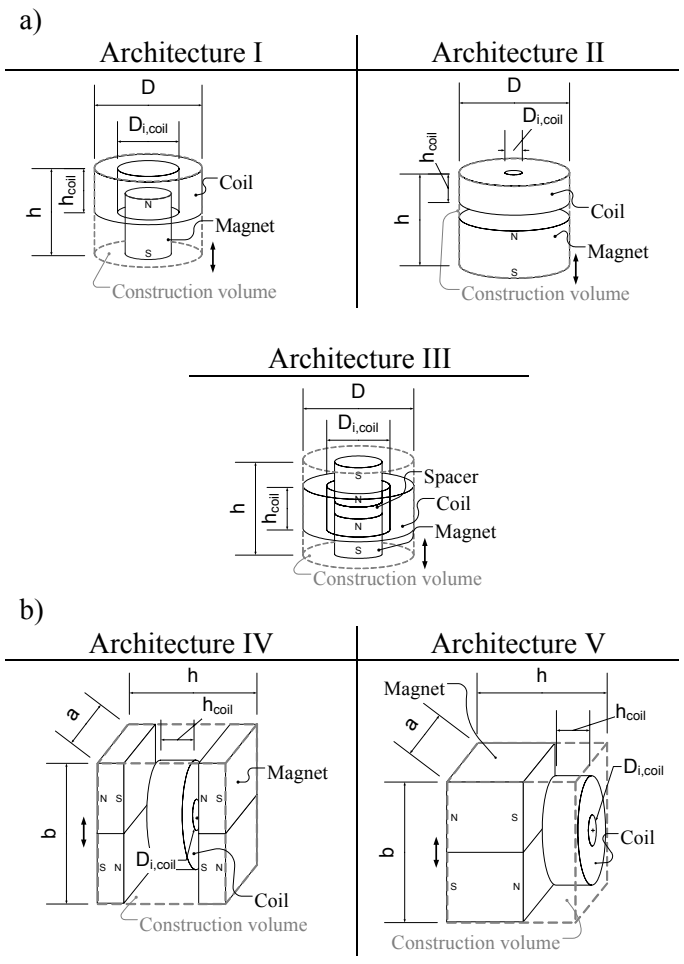


*Fig. 1: a) "Magnet in–line coil" architectures and b) "Magnet across coil" architectures*

dimension for each architecture is simply obtained by varying the geometric parameters of coil and magnet in the construction volume. In a final step the optimal voltage and power levels are compared to each other. With the presented results the designer of electromagnetic vibration transducers gets a guideline which architecture to choose for practical voltage and power levels, respectively.

## 2. BOUNDARY CONDITIONS AND OPTIMIZATION PROCEDURE

The first goal of the optimization is to maximize the voltage and power output of the architectures (in the following abbreviated arch). Because the quantitative comparison of each arch is another intention of the presented work, it is important to declare overall fixed boundary conditions (Tab. 1). For the presented results values similar to mesoscale vibration transducers have been used. The construction volume $V_{\mathrm{constr}}$ (cylinder resp. cuboid) contains the coil and the magnet at its equilibrium point. In the first step of the optimization procedure (Fig. 2) two geometry vectors for the inner coil diameter ($D_{\mathrm{i,coil}}$) and the coil height ($h_{\mathrm{coil}}$) are defined. With the fixed gap between coil and magnet the geometry of the magnet follows. In this regard the only exception is arch I where the depth of immersion has to be taken into account too [1]. Afterwards the windings and internal resistance of the Coil can be calculated as:

$$N_{long} = \frac{2 \cdot h_{coil}}{D_{co}\sqrt{\pi / k_{co}}},$$
$$N_{lat} = \frac{2 \cdot (D - D_i)/2}{D_{co}\sqrt{\pi / k_{co}}}, \qquad (1)$$
$$R_{in} = N_{long} \cdot N_{lat} \cdot 2\pi \frac{(D - D_i)}{4} \cdot R'.$$

The magnetic field (cylindrical and rectangular magnets) is calculated using the scalar potential model [2, 3]. Due to lack of space the formulas for the magnetic field have been left out, but it is essential to know that they contain elliptic integrals which have to be solved numerically. These results are than used to compute the total magnetic flux $\varphi$ in the coil (at the equilibrium point of the oscillating magnet) and its gradient:

$$\varphi = \sum_{N_{long}} \sum_{N_{lat}} \int_{A_{i,j}} \vec{B} d\overrightarrow{A_{i,j}},$$
$$K = (d\varphi / dx)_{equi}. \qquad (2)$$

Therein $A_{\mathrm{i,j}}$ indicates the area enclosed by the respective Winding. With the internal resistance and

*Table 1: Overall boundary conditions applied for optimization calculations*

| Symbol | Description | Value | Unit |
|---|---|---|---|
| | ***Geometry*** | | |
| $V_{\mathrm{constr}}$ | Construction volume | 1 | cm³ |
| $G$ | Gap (Coil/Magnet) | 0.5 | mm |
| $Z_{\max}$ | Maximum displacement | 1 | mm |
| | ***Magnet*** | | |
| $B_{\mathrm{r}}$ | Remanenz | 1.1 | T |
| $\rho$ | Density of magnet | 7.6 | g/cm³ |
| | ***Coil*** | | |
| $k_{\mathrm{co}}$ | Copper fill factor | 0.6 | 1 |
| $D_{\mathrm{co}}$ | Wire diameter | 40 | µm |
| $R'$ | Resistance per unit length | 13.6 | Ω/m |
| | ***Other*** | | |
| $Y$ | Excitation amplitude | 10 | m/s² |
| $f$ | Excitation frequency | 100 | Hz |
| $c_{\mathrm{m}}$ | Mechanical damping | 0.1 | N/m/s |

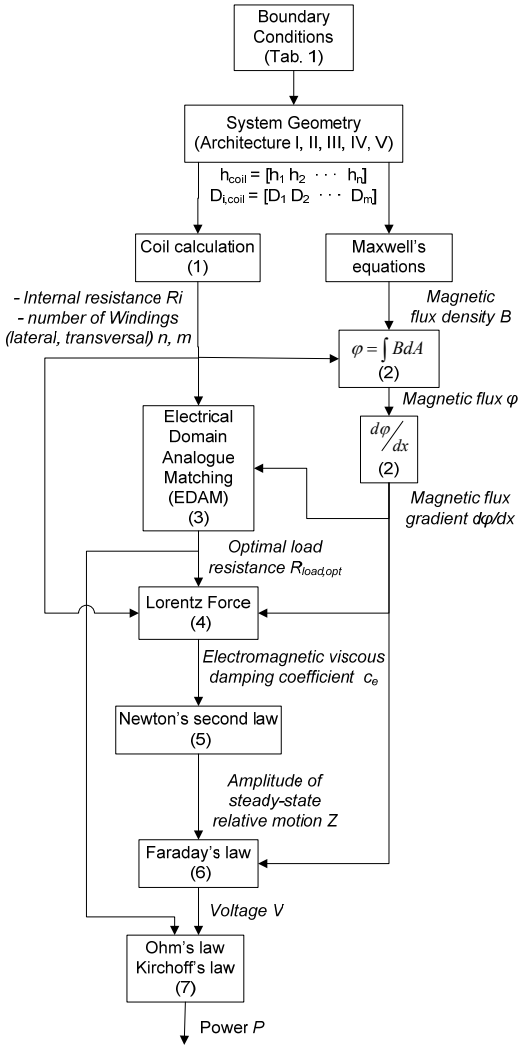


*Fig. 2: Procedural structure of the optimization approach*

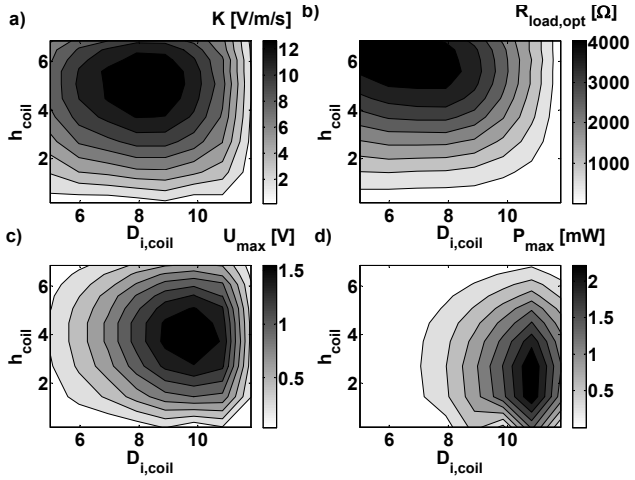


*Fig. 3: Optimization result for "Magnet in–line coil" architecture I.*

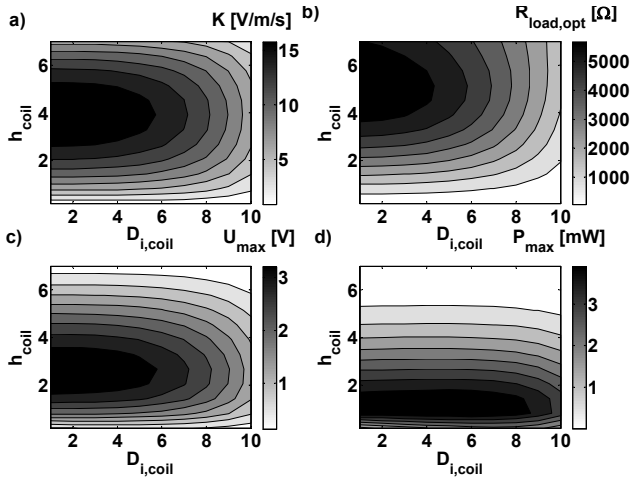


*Fig. 4: Optimization result for "Magnet in–line coil" architecture II*

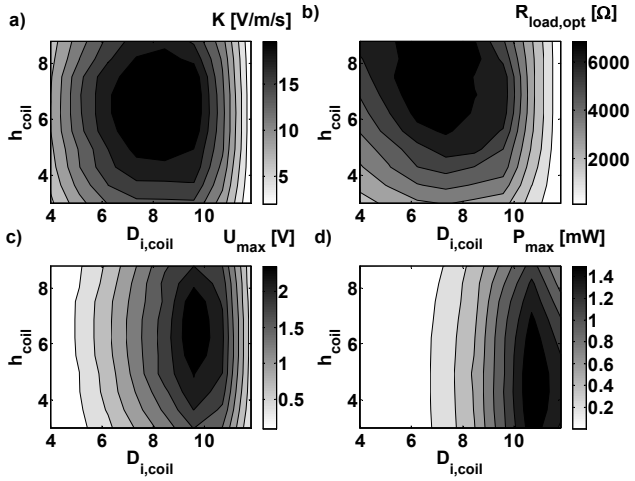


*Fig. 5: Optimization result for "Magnet in–line coil" architecture III*

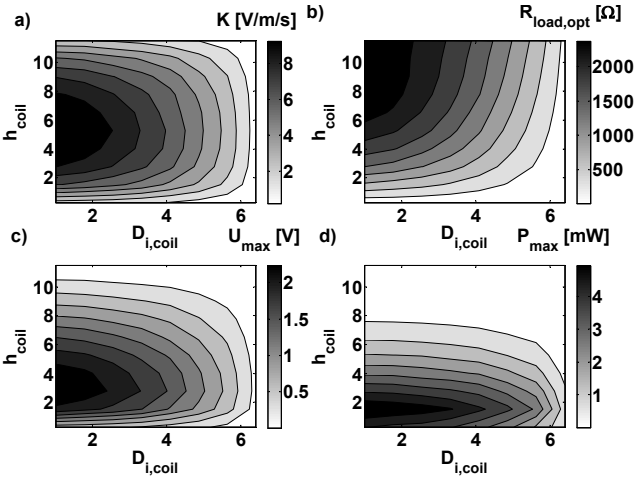


*Fig. 6: Optimization result for "Magnet across coil" architecture IV*

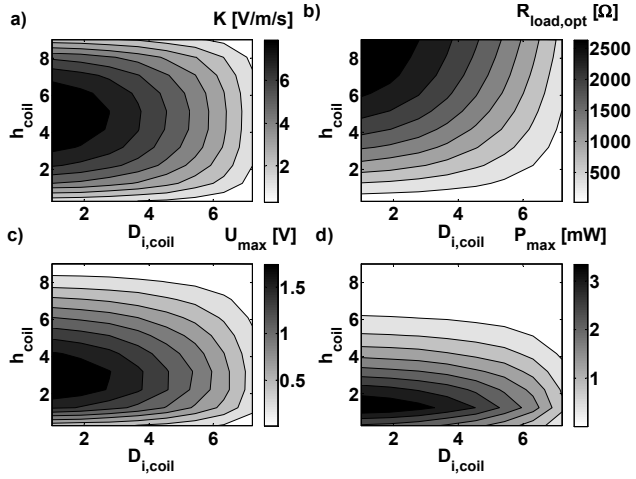


*Fig. 7: Optimization result for "Magnet across coil" architecture V*

the magnetic flux gradient the optimal load resistance can be determined [4]:

$$R_{load,opt} = R_{in} + \frac{K^2}{c_m}. \tag{3}$$

This result is in turn necessary to determine the electromagnetic damping coefficient:

$$c_e = \frac{K^2}{\left(R_{in} + R_{load,opt}\right)}. \tag{4}$$

Next the relative amplitude of steady-state motion can be calculated:

$$Z = \frac{m\omega^2 Y}{\sqrt{\left(k - m\omega^2\right)^2 + \left(\left(c_e + c_m\right)\omega\right)^2}}, \tag{5}$$

where $k$ indicates the spring constant yielding the resonance frequency defined in the boundary conditions. Using Faraday's law of induction the EMF (electromotive force) is given as:

$$\varepsilon = -\frac{d\varphi}{dt} = -\left(\frac{dA}{dt}B + \frac{dB}{dt}A\right) = -\frac{d\varphi}{dz}\cdot\frac{dz}{dt}. \quad (6)$$

In order to obtain the output power Ohm's law and Kirchhoff's law has to be applied to the simple resistive load considered here:

$$V_{R_{load,opt}} = \varepsilon \cdot \left(\frac{R_{load,opt}}{R_{load,opt} + R_{in}}\right), \quad (7)$$

$$P_{R_{load,opt}} = \frac{V_{R_{load,opt}}^{2}}{R_{load,opt}}.$$

Note that the inductance of the coil has been neglected because the reactance we want to consider is much smaller than the resistance. The optimization procedure following from (1) – (7) is applied to every pair of variables of the two geometry vectors. In order to understand the advantage and disadvantage of each arch the optimal load resistance and magnetic flux gradient has been recorded beyond the maximum voltage and power output.

## 3. OPTIMIZATION RESULTS AND DISCUSSION

The results of the optimization for arch I – V are shown in Fig. 3 – 7. In each figure a) illustrates the magnetic flux gradient at equilibrium point, b) the optimal load resistance, c) the maximal output voltage and d) the maximal output power. As it can be seen for example in Fig. 3a the magnetic flux gradient has an optimum ($D_{i,coil}$ = 8 mm, $h_{coil}$ = 5 mm), but for the EMF the velocity (high inner displacement due to high oscillating mass) has to be taken into account too. That's why the optimum for EMF voltage (Fig. 3c) is shifted to higher values of $D_{i,coil}$ and smaller values of $h_{coil}$ respectively (bigger magnet!). Since a bigger magnet implies a smaller coil and smaller resistance as well the optimum of the output power is shifted to even higher values of $D_{i,coil}$ and smaller values of $h_{coil}$ (Fig. 3d). This effect is obvious for arch III too. In this regard the only difference for arch II, IV and V is that the magnet size is not dependent on $D_{i,coil}$. Therefore the EMF voltage steadily increases for smaller $D_{i,coil}$ which has been limited to 1 mm. The importance of the mass is best observable for arch III [5]. Here the greatest magnetic flux gradient can be achieved but due to the comparatively small magnet the maximum output power (and voltage) is nevertheless quite low compared to arch II, for example. From all arch it is apparent that there exists a separate optimum for voltage and power. Which point to choose depends on whether high output voltage or power levels are desired. As an essential summary highest voltage levels are expected for arch II and greatest power with arch IV. The values of voltage and power at the optimum points are shown in Fig. 8.

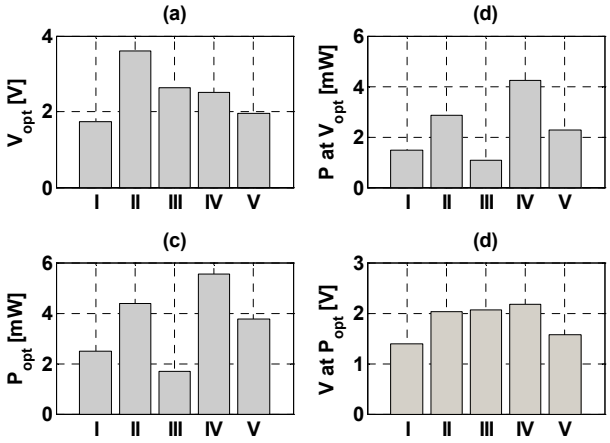


*Fig. 8: Comparison of maximal values of EMF voltage (a), power at maximal voltage point (b), maximal output power (c) and voltage at maximal output power point (d)*

## ACKNOWLEDGEMENTS

The authors want to acknowledge the funding of the ZOFF III project "Energieeffiziente Autonome Mikrosysteme" by the government of Baden-Württemberg

## REFERENCES

[1] D. Spreemann, D. Hoffmann, B. Folkmer, Y. Manoli: *Numerical Optimization Approach for Resonant Electromagnetic Vibration Transducer Designed for Random Vibration,* to be published in PowerMEMS 2008 special issue in JMM

[2] K. Foelsch: *Magnetfeld und Induktivität einer zylindrischen Spule,* Archiv für Elektrotechnik, XXX. Band. 3. Heft, 1936

[3] X. Gou, Y. Yang, X. Zheng: *Analytic Expression of magnetic field distribution of rectangular permanent magnets,* Applied Mathematics and Mechanics, Vol. 25. No. 3, March 2004

[4] N.G. Stephen: *On energy harvesting from ambient vibration,* Journal of Sound and Vibration, Vol. 293, pp. 409-425, 2006

[5] T. von Büren, G. Tröster: *Design and optimization of a linear vibration-driven electromagnetic micro-power generator*, Sensors and Actuators A 135, pp 765-775, 2006